CHEMISTRY
A EUROPEAN JOURNAL

DOI: 10.1002/chem.200903216

Evidence for Drug Release from a Metalla-Cage Delivery Vector Following Cellular Internalisation

Olivier Zava,[a] Johan Mattsson,[b] Bruno Therrien,*[b] and Paul J. Dyson*[a]

One of the main challenges in cancer chemotherapy is to develop drugs that selectively target cancer cells in order to reduce general toxicity and consequently side effects. One such targeting method involves using large carrier compounds that release a drug once inside a cancer cell, since large compounds selectively accumulate in cancer tissue due to the "enhanced permeability and retention effect".[1] Recently, we have shown that the encapsulation of a hydrophobic metallo-drug guest in a water-soluble hexacationic arene ruthenium cage delivery vector produces a synergistic effect, due to the modest cytotoxicity of the cage itself, and the cytotoxicity of the encapsulated guest compound.[2] We have now encapsulated in the cavity of $[Ru_6(p\text{-}i\text{Pr}C_6H_4Me)_6(tpt)_2(C_6H_2O_4)_3]^{6+}$ (**1**) (tpt = 2,4,6-tris(pyridin-4-yl)-1,3,5-triazine), an intrinsically fluorescent pyrenyl compound (pyrene-R = 1-(4,6-dichloro-1,3,5-triazin-2-yl)pyrene), thus giving rise to the hexanuclear metalla-prism $[\text{pyrene-R}\subset\mathbf{1}]^{6+}$, in which the pyrenyl derivative occupies the cavity of **1**. The fluorescence of pyrene-R is quenched inside the metalla-prism cavity. A study of this new system has provided direct evidence that once inside the cell, the hexaruthenium cage releases the fluorescent guest, thus confirming our initial hypothesis that cage **1** can act as a Trojan horse for cancer cells.[2] In addition, experiments into the uptake mechanism indicate that an assisted diffusion pathway is in operation.

The encapsulation of guest molecules in coordinationally driven self-assembled cage compounds has been extensively studied.[3] The encapsulation process depends on the complementary of the guest's size, shape, and chemical surface with respect to that of the host cavity. Potential applications of these systems have been found in chemistry (recognition and selective transformations), biology (translocation of drugs across membranes, sensors, biomimetics), and material science (construction of macroscopic architectures for storage and devices at the molecular level).[3]

Additionally, ruthenium complexes have considerable potential in a number of biomedical applications such as diagnostics and therapeutics and a wide range of ruthenium compounds have been evaluated as putative anticancer agents.[4] Two ruthenium compounds have even completed phase I clinical trials.[5,6] The biological properties of ruthenium complexes have been extensively studied, with a focus on how such compounds interact with DNA,[7] and they are known to enter the cells through various pathways.[8,9] Consequently, a cage built with cell permeate ruthenium complexes could be a vehicle of choice for hydrophobic molecules.

The synthesis of the metalla-cage compound $[\text{pyrene-R}\subset\mathbf{1}]^{6+}$ encapsulating 1-(4,6-dichloro-1,3,5-triazin-2-yl)pyrene (pyrene-R) follows a two step strategy in which the dinuclear 2,5-dihydroxy-1,4-benzoquinonato ($C_6H_2O_4$) complex $[Ru_2(p\text{-}i\text{Pr}C_6H_4Me)_2(C_6H_2O_4)Cl_2]$ is used as a bi-metallic connector (See Scheme 1).[2] The hexacationic carceplex system is isolated in good yield and characterised as the triflate salt, $[\text{pyrene-R}\subset\mathbf{1}][CF_3SO_3]_6$. The ^{1}H NMR spectrum of $[\text{pyrene-R}\subset\mathbf{1}]^{6+}$ in [D$_6$]acetone shows broad signals for the protons of the encapsulated pyrenyl derivative as well as for the cage protons. The chemical shifts observed for both pyrene-R and cage $\mathbf{1}^{6+}$ are consistent with the encapsulation of a functionalised pyrenyl derivative.[10] The encapsulation of pyrene-R in $\mathbf{1}^{6+}$ is further confirmed by ESI-MS in which peaks corresponding to $[\text{pyrene-R}\subset\mathbf{1}+(CF_3SO_3)_3]^{3+}$ and $[\text{pyrene-R}\subset\mathbf{1}+(CF_3SO_3)_2]^{4+}$ are observed at *m/z* 1081.4 and 773.8, respectively.

To determine appropriate working concentrations for subsequent investigations, the cytotoxicity of the different compounds, pyrene-R, $[\mathbf{1}][CF_3SO_3]_6$, and $[\text{pyrene-R}\subset\mathbf{1}][CF_3SO_3]_6$, were determined. As shown in Table 1, pyrene-R alone does not show any measurable IC_{50} value at the con-

[a] Dr. O. Zava, Prof. Dr. P. J. Dyson
Institut des Sciences et Ingénierie Chimique
Ecole Polytechnique Fédérale de Lausanne (EPFL)
1015 Lausanne (Switzerland)
Fax: (+41) 21-693-9854
E-mail: paul.dyson@epfl.ch

[b] J. Mattsson, Dr. B. Therrien
Institut de Chimie, University of Neuchatel
Case postale 158, 2009, Neuchatel (Switzerland)
Fax: (+41) 32-7182511
E-mail: bruno.therrien@unine.ch

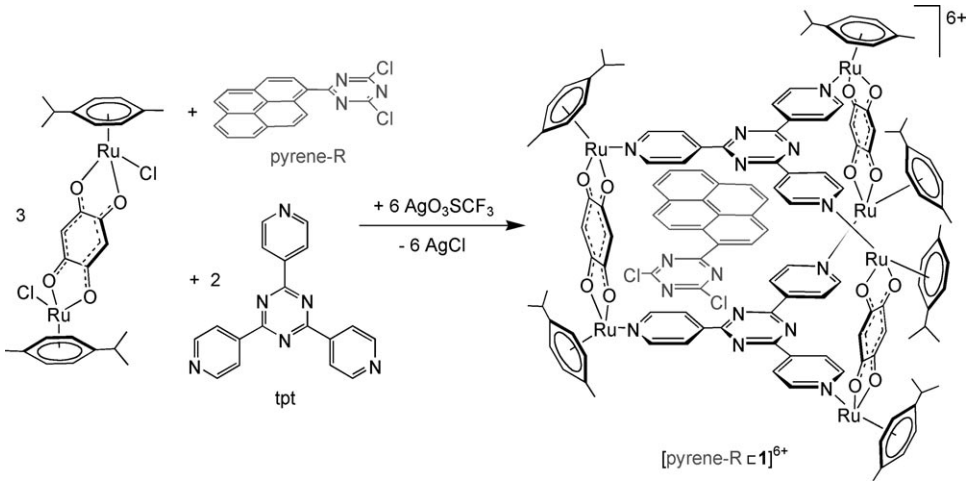

Scheme 1. Synthesis of [pyrene-R⊂**1**][CF_3SO_3]$_6$.

Table 1. Cytotoxicity of pyrene-R, [**1**]$^{6+}$ and [pyrene-R⊂**1**]$^{6+}$ in human ovarian A2780 cancer cells.[a]

Compound	IC_{50} (μM)
pyrene-R	>20
[**1**][CF_3SO_3]$_6$	16±2.3
[pyrene-R⊂**1**][CF_3SO_3]$_6$	6±0.8

[a] Experiments were conducted in triplicate wells and repeated twice.

centrations used (up to 20 μM), whereas the cage compound **1**$^{6+}$ showed a moderate cytotoxicity on human ovarian A2780 cancer cells. However, [pyrene-R⊂**1**]$^{6+}$ shows enhancement of its activity as compared to the empty cage, suggesting that the cage facilitates uptake of the poorly soluble pyrene-R compound into the cells.

Based on these results, we studied the uptake of pyrene-R and [pyrene-R⊂**1**]$^{6+}$, taking advantage of the natural fluorescence of pyrene-R. Interestingly, as shown in Figure 1 the pyrene-R inside the cage does not show fluorescence at pH 2 or pH 7, but at pH 12 it exhibits the typical fluorescence of pyrene-R alone. The cage compound **1**$^{6+}$ does not show any fluorescence when excited at 350 nm (data not shown). This would suggest that once trapped inside the cage the fluorescence of the pyrene-R guest molecule is quenched and upon destruction of the cage complex at pH 12, the fluorescence is due to free pyrene-R.

Accordingly, the free pyrene-R was tracked by fluorescence microscopy following incubation with A2780 cells (Figure 2). An increase of fluorescence is observed inside the cells following treatment with [pyrene-R⊂**1**]$^{6+}$, whereas treatment with pyrene-R at the same concentration only shows a modest effect. It is also noteworthy that for [pyrene-R⊂**1**]$^{6+}$ accumulation in cytoplasmic organelles is observed.

Recently, Puckett et al. used flow cytometry to quantify the uptake of a fluorescent polypyridyl ruthenium compound.[8] We exploited their technique to confirm the data obtained by microscopy and provide a more quantitative picture. Figure 3 shows typical histograms obtained from the fluorescence of cells treated with pyrene-R and [pyrene-R⊂**1**]$^{6+}$. These data confirm the higher fluorescence of cells treated with the encapsulated pyrene-R in **1** and allowed the uptake of the fluorophore to be quantitatively assessed.

Small molecules can enter cells in multiple ways, including active, that is, energy-dependent (endocytosis), or energy-independent phenomena (passive diffusion or assisted diffusion).[8,11,12] To provide insights

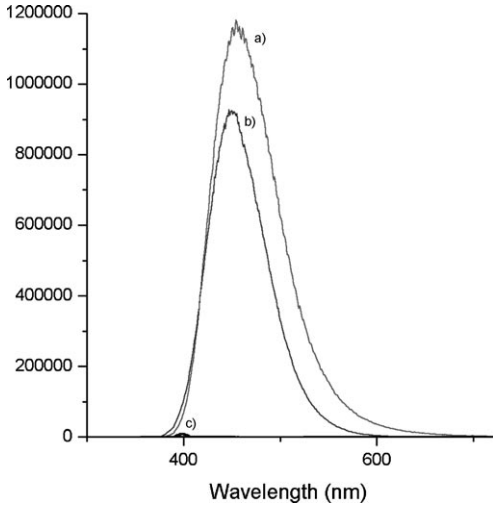

Figure 1. Fluorescence spectra of pyrene-R and [pyrene-R⊂**1**]$^{6+}$ at various pH, from 2 to 12. a) Fluorescence spectrum of pyrene-R at pH 12; b) fluorescence spectrum of [pyrene-R⊂**1**]$^{6+}$ at pH 12; c) fluorescence spectra of [pyrene-R⊂**1**]$^{6+}$ at pH 2 and 7 which do not show significant fluorescence.

into the uptake mechanism, the mean fluorescence, and accordingly the uptake/release of pyrene-R, as a function of concentration and time was monitored during incubation with [pyrene-R⊂**1**]$^{6+}$ and during chase (Figure 4). Figure 4 (top) shows that the uptake of the cage does not increase linearly with incubation time. This observation implies that, at least in part, the cellular machinery is involved, for example, membrane transporters or receptors that limited the rate of uptake. This inference is confirmed by the fact that the fluorescence of the cell does not follow linearly with the concentration of [pyrene-R⊂**1**]$^{6+}$ (Figure 4, middle). Nevertheless, at the concentrations tested it is not possible to determine if the uptake reaches a plateau or increases linearly at higher concentrations. Thus we cannot completely exclude a passive component in the mechanism of uptake,[12]

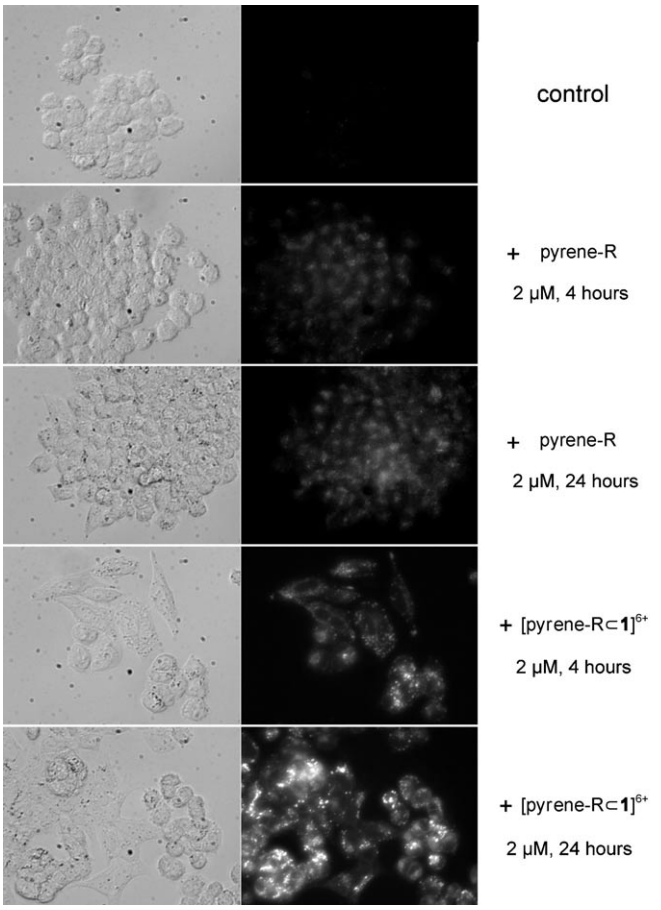

Figure 2. Microscopy images of cells incubated with pyrene-R, $[\mathbf{1}]^{6+}$ and $[\text{pyrene-R}\subset\mathbf{1}]^{6+}$, transmitted light (left) and fluorescent light (right).

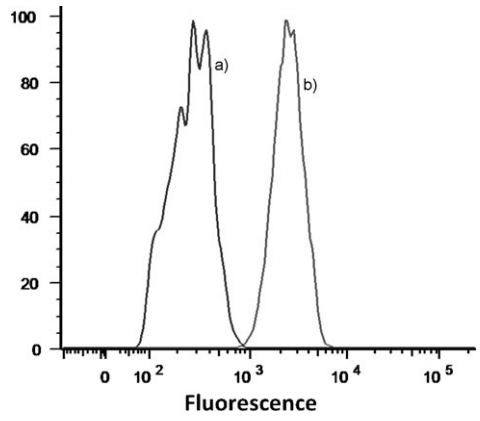

Figure 3. Flow cytometry analysis of the fluorescence of the A2780 cells treated with $[\text{pyrene-R}\subset\mathbf{1}]^{6+}$ (a) and pyrene-R alone (b).

although an assisted diffusion pathway fits best with the obtained data. It is worth noting that at 4 °C neither uptake nor chase of pyrene-R seems to be significantly altered compared to the values obtained at 37 °C. Hence endocytosis may be disqualified as uptake does not require energy.

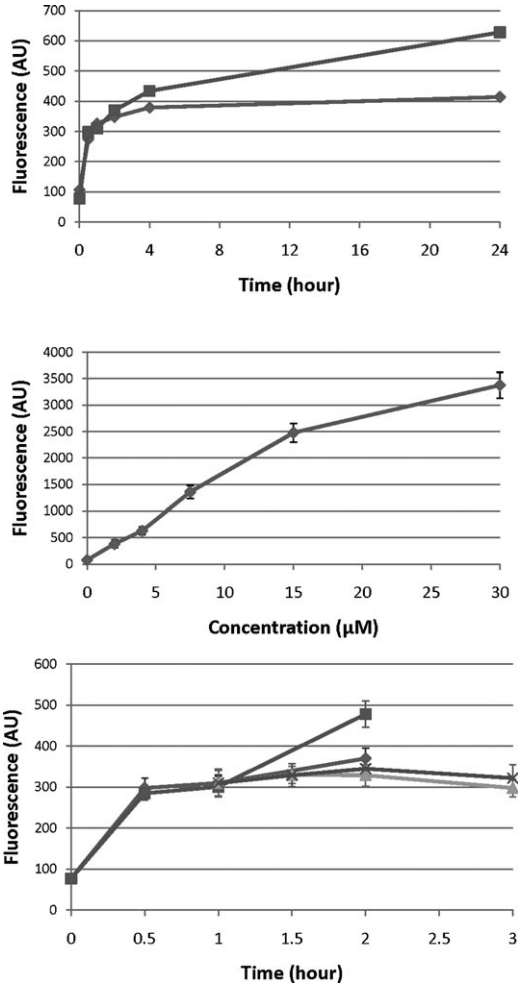

Figure 4. Influence of various treatments on the fluorescence of cells treated with $[\text{pyrene-R}\subset\mathbf{1}]^{6+}$. The mean fluorescence of the cells was quantified by flow cytometry. Top: Time course of release of pyrene-R in cells treated with 2 or 4 μM of $[\text{pyrene-R}\subset\mathbf{1}]^{6+}$ (■ and ▲, respectively). Middle: Concentration dependency of the release of pyrene-R in cells treated with $[\text{pyrene-R}\subset\mathbf{1}]^{6+}$. Bottom: Monitoring of pyrene-R fluorescence during uptake at either 37 °C or 4 °C (◆ and ■, respectively) and during chase after 1 hour incubation with 4 μM of $[\text{pyrene-R}\subset\mathbf{1}]^{6+}$ at 37 °C or 4 °C (▲ and ×, respectively).

In conclusion, direct evidence for the efficient release of a hydrophobic molecule from a metalla-cage following uptake into a cell is provided. Employing a fluorescent molecule as a cargo we have been able to increase its cytotoxicity, increase its cellular uptake and to monitor its accumulation in the cells by microscopy and flow cytometry. Furthermore, these results suggest that the entry of the compound into the cell is, at least in part, dependent on an assisted diffusion pathway. This mode of uptake has been described for cisplatin[13] and other platinum-based drugs,[14] for which potential transporters have been identified.[15] The existence of a facilitated mode of entry into cells implies a certain cell specificity, which offers a potential advantage for the use of such a delivery vehicle in medicinal applications.[15]

Experimental Section

All organic solvents were degassed and saturated with nitrogen prior to use. 1-(4,6-Dichloro-1,3,5-triazin-2-yl)pyrene (pyrene-R) was purchased from Fluka. 2,4,6-Tris(pyridin-4-yl)-1,3,5-triazine (tpt)[16] and $[Ru_2(p\text{-}iPrC_6H_4Me)_2(C_6H_2O_4)Cl_2]$[1] were prepared according to published methods. NMR spectra were recorded on a Bruker 400 MHz spectrometer. IR spectra were recorded on a Perkin–Elmer 1720X FT-IR spectrometer (4000–400 cm^1). Microanalyses were performed by the Laboratory of Pharmaceutical Chemistry, University of Geneva (Switzerland). Electrospray mass spectra were obtained in positive-ion mode with an LCQ Finnigan mass spectrometer.

[pyrene-R⊂1][CF_3SO_3]$_6$: A mixture of $[Ru_2(p\text{-}iPrC_6H_4Me)_2(C_6H_2O_4)Cl_2]$ (50 mg, 0.075 mmol) and $AgCF_3SO_3$ (40 mg, 0.16 mmol) in MeOH (20 mL) was stirred for 2 h, then filtered. Next, tpt (15 mg, 0.05 mmol) and 1-(4,6-dichloro-1,3,5-triazin-2-yl)pyrene (11 mg, 0.03 mmol) were added to the red filtrate. The mixture was stirred at RT overnight and the solvent was removed under vacuum. The dark residue was re-dissolved in CH_2Cl_2 (20 mL) and after filtration, the solution was concentrated (5 mL), and diethyl ether was added to precipitate the red solid. Yield 59 mg, 65%; ^{1}H NMR (400 MHz, [D$_6$]acetone, 25°C): $\delta = 8.54$ (br, 12H; H_α), 8.00 (br, 12H; H_β), 6.20 (d, $^3J(H,H) = 6.0$ Hz, 12H; H_{ar}), 6.18 (s, 6H; H_q), 5.98 (d, $^3J(H,H) = 6.0$ Hz, 12H; H_{ar}), 2.97 (sept, $^3J(H,H) = 6.7$ Hz, 6H; CH), 2.21 (s, 18H; CH_3), 1.39 ppm (d, $^3J(H,H) = 6.7$ Hz, 36H; CH_3); ^{13}C {^{1}H} NMR (100 MHz, [D$_6$]acetone, 25°C): $\delta = 184.37$, 154.07, 124.31, 104.25, 102.19, 99.34, 83.93, 82.37, 31.29, 21.69, 17.31 ppm; IR (KBr): $\tilde{\nu} =$ 1523 (s), 1377 (s), 1258 (s), 1224 (w), 1159 (w), 1030 (m), 811 (w), 638 cm^{-1} (w); ESI-MS: *m/z* (%): 1081.4 (100) [pyrene-R⊂**1**+$(CF_3SO_3)_3]^{3+}$, 773.8 (35) [pyrene-R⊂**1**+$(CF_3SO_3)_2]^{4+}$; elemental analysis calcd (%) for $C_{139}H_{123}Cl_2F_{18}N_{15}O_{30}Ru_6S_6$: C 45.18, H 3.36, N 5.69; found: C 44.83, H 3.19, N 5.93.

Cell culture and inhibition of cell growth: Human A2780 ovarian carcinoma cells were obtained from the European Centre of Cell Cultures (ECACC, Salisbury, UK) and maintained in culture as described by the provider. The cells were routinely grown in RPMI 1640 medium containing 10% foetal calf serum (FCS) and antibiotics at 37°C and 6% CO_2. For the evaluation of growth inhibition tests, the cells were seeded in 96-well plates and grown for 24 h in complete medium. Complexes were added to the required concentration and added to the cell culture for 72 h incubation. Solutions of the compounds were applied by diluting a freshly prepared stock solution of the corresponding compound in DMSO, with the final concentration of < 0.05% in the medium. The MTT test was performed in the last 2 h without changing the culture medium. Following drug exposure, MTT (Sigma) was added to the cells at the final concentration of 0.2 mg mL^{-1} and incubated for 2 h, then the culture medium was aspirated and the violet formazan precipitate dissolved in DMSO. The optical density was quantified at 540 nm using a multiwell plate reader (iEMS Reader MF, Labsystems, US), and the percentage of surviving cells was calculated from the ratio of the absorbance of treated to untreated cells. The IC_{50} values for the inhibition of cell growth were determined by fitting the plot of the percentage of surviving cells against the drug concentration using a sigmoidal function (Origin v7.5).

Microscopy experiments: Cells were grown for 24 h on chambered coverglass slides (Lab-Tek, NUNC) in complete medium at the density of 1.10^4 and then exposed to the appropriate compounds at 37°C in the dark. Excess complex was removed with PBS, fixed with 4% formaldehyde in PBS for 30 min in the dark and rinsed twice with PBS before observation. Cells were mounted in PBS before being observed by fluorescence microscopy using a Zeiss Axiovert 200 M microscope equipped with a 40X air immersion objective. Filters used for excitation and detection of DAPI were 345 nm and 448 nm, respectively. Fluorescence signal intensities were evaluated using MetaMorph software.

Flow cytometry: Cells were detached from culture with EDTA (0.48 mM in PBS) and incubated at 1×10^6 cells mL^{-1} with the compound (added from a concentrated DMSO stock solution), under conditions described above, and then placed on ice. The fluorescence of ≈20000 cells was measured using a BD LSR II analyser, exciting with the 355 nm laser for pyrene-R. Emission was observed at 450/40 nm. Fluorescence data were analysed using the FlowJo 8 software. Fluorescence data are reported as the mean.

Acknowledgements

This work is supported by the Fonds National Suisse de la Recherche Scientifique. A generous loan of ruthenium trichloride hydrate from Johnson Matthey Technology Centre is gratefully acknowledged.

Keywords: anticancer agents · drug delivery · in vitro assays · ruthenium · supramolecular chemistry

[1] D. F. Baban, L. W. Seymour, *Adv. Drug Delivery Rev.* **1998**, *34*, 109–119.
[2] B. Therrien, G. Süss-Fink, P. Govindaswamy, A. K. Renfrew, P. J. Dyson, *Angew. Chem.* **2008**, *120*, 3833–3836; *Angew. Chem. Int. Ed.* **2008**, *47*, 3773–3776.
[3] a) D. L. Caulder, K. N. Raymond, *Acc. Chem. Res.* **1999**, *32*, 975–982; b) F. Hof, S. L. Craig, C. Nuckolls, J. Rebek, Jr., *Angew.Chem.* **2002**, *114*, 1556–1578; *Angew.Chem. Int. Ed.* **2002**, *41*, 1488–1508; c) T. B. Rauchfuss, K. Severin in *Organic Nanostructures* (Eds.: J. L. Atwood, J. W. Steed), Wiley-VCH, Weinheim, **2008**, pp. 179–203; d) M. D. Ward in *Organic Nanostructures* (Eds.: J. L. Atwood, J. W. Steed), Wiley-VCH, Weinheim, **2008**, pp. 223–250; e) M. Yoshizawa, J. K. Klosterman, M. Fujita, *Angew. Chem.* **2009**, *121*, 3470–3490; *Angew. Chem. Int. Ed.* **2009**, *48*, 3418–3438; f) P. J. Stang, *J. Org. Chem.* **2009**, *74*, 2–20; g) Y.-F. Han, W.-G. Jia, Y.-J. Lin, G.-X. Jin, *Angew. Chem.* **2009**, *121*, 6352–6356; *Angew. Chem. Int. Ed.* **2009**, *48*, 6234–6238.
[4] a) P. J. Dyson, G. Sava, *Dalton Trans.* **2006**, 1929–1933; b) A. Levina, A. Mitra, P. A. Lay, *Metallomics* **2009**, *1*, 458–470; c) G. Süss-Fink, *Dalton Trans.* **2010**, DOI: 10.1039/b916860p.
[5] J. M. Rademaker-Lakhai, D. van den Bongard, D. Pluim, J. H. Beijnen, J. H. M. Schellens, *Clin. Cancer Res.* **2004**, *10*, 3717–3727.
[6] C. G. Hartinger, S. Zorbas-Seifried, M. A. Jakupec, B. Kynast, H. Zorbas, B. K. Keppler, *J. Inorg. Biochem.* **2006**, *100*, 891–904.
[7] a) V. Brabec, O. Nováková, *Drug Resist. Updates* **2006**, *9*, 111–122; b) H. C. Feng Gao, L.-N. Ji, *Chem. Biodiversity* **2008**, *5*, 1962–1979.
[8] C. A. Puckett, J. K. Barton, *Biochem. J.* **2008**, *409–416*, 11711–11716.
[9] a) F. Schmitt, P. Govindaswamy, G. Süss-Fink, W. H. Ang, P. J. Dyson, L. Juillerat-Jeanneret, B. Therrien, *J. Med. Chem.* **2008**, *51*, 1811–1816; b) O. Zava, S. M. Zakeeruddin, C. Danelon, H. Vogel, M. Grätzel, P. J. Dyson, *ChemBioChem* **2009**, *10*, 1796–1800.
[10] a) J. Mattsson, P. Govindaswamy, J. Furrer, Y. Sei, K. Yamaguchi, G. Süss-Fink, B. Therrien, *Organometallics* **2008**, *27*, 4346–4356; b) N. P. E. Barry, B. Therrien, *Eur. J. Inorg. Chem.* **2009**, 4695–4700.
[11] O. Briz, M. A. Serrano, N. Rebollo, B. Hagenbuch, P. J. Meier, H. Koepsell, J. J. Marin, *Mol. Pharmacol.* **2002**, *61*, 853–860.
[12] D. L. Bourdet, D. R. Thakker, *Pharm. Res.* **2006**, *23*, 1165–1177.
[13] a) A. K. Holzer, K. Katano, L. W. Klomp, S. B. Howell, *Clin. Cancer Res.* **2004**, *10*, 6744–6749; b) G. V. Kalayda, C. H. Wagner, I. Buss, J. Reedijk, U. Jaehde, *BMC Cancer* **2008**, *8*, 175.
[14] M. D. Hall, M. Okabe, D. W. Shen, X. J. Liang, M. M. Gottesman, *Annu. Rev. Pharmacol. Toxicol.* **2008**, *48*, 495–535.
[15] P. D. Dobson, D. B. Kell, *Nat. Rev. Drug Discovery* **2008**, *7*, 205–220.
[16] H. L. Anderson, S. Anderson, J. K. M. Sanders, *J. Chem. Soc. Perkin Trans. 1* **1995**, 2231–2246.

Received: November 24, 2009
Published online: December 23, 2009

